

$\chi^{(2)}$ Grating in Ru Derivative Chromophores Incorporated within the PMMA Polymer Matrices

A. Migalska-Zalas, Z. Sofiani, and B. Sahraoui

Université d'Angers, laboratoire POMA UMR CNRS 6136, 2. Bd Lavoisier, 49045 Angers, France

I. V. Kityk* and S. Tkaczyk

Institute of Biology and Biophysics, Technical University of Częstochowa, Al. Armii Krajowej 36, Częstochowa, Poland, and Institute of Physics WSP Częstochowa, PL-42217, Al. Armii Krajowej 13/15, Częstochowa, Poland

V. Yuvshenko

Institute of Physics, Ukrainian Academy of Science, Kyjiv, pr. Nauki 144, Ukraine

J.-L. Fillaut and J. Perruchon

Institut de chimie de Rennes, Université Rennes I- UMR CNRS 6509, Laboratoire Organométalliques et Catalyse, 35042 Rennes Cedex, France

T. J. J. Muller

Organisch-Chemisches Institut, Universität Heidelberg, 69120 Heidelberg, Germany

Received: March 18, 2004; In Final Form: July 11, 2004

We have found that Ru derivative chromophores incorporated into the PMMA polymer matrices might be considered as promising materials for optical poling. The maximally achieved effective second-order optical susceptibility for the wavelength 1.89 μm is about 1.94 pm/V. The investigated composites possess metastable trapping levels originating both from the d states of Ru and due to effective charge transfer due to the presence of π -conjugated states. Because of incorporation of the chromophore into polymer matrices, we have revealed that the maximal susceptibility is observed at 5–6% of the chromophore in weighting units. The further increase of the second-order susceptibility is limited by the appearance of chromophore agglomerates substantially restraining second-order susceptibilities. The investigated composites possess long-lived $\chi^{(2)}$ grating, which decreases less than 76% after 600 min of laser treatment. The electrostatic field causes additional reanimation of the second harmonic generation during the decay regime. The electron microscopy pictures clearly confirm appearance of the $\chi^{(2)}$ grating.

I. Introduction

The second harmonic generation (SHG) described by third-rank polar tensors is generally forbidden by symmetry in randomly disordered media. However, in 1980, Fujii et al. showed¹ the possibility for weak SHG in the disordered media. In ref 2, the effect of breaking the randomly oriented centrosymmetry is slightly understandable for the near-the-surface states;³ however, it is difficult to expect an occurrence of the bulk noncentrosymmetry, which is a necessary attribute of the $\chi^{(2)}$ grating. The first disordered optical materials in which SHG was observed were optical fibers. However, physical insight of the observed effect was not so simple to explain.^{4,5} There appeared several theoretical approaches, particularly in ref 4; it was shown that there occurs static polarization (see eq 1) and the associated static electric field might be described by eq 2

$$P_i^0 = \chi_{ijkl}^3 E_j E_k E_l \quad (1)$$

$$E_i^0 = 4\pi P_i^0 \quad (2)$$

where the particular parameters correspond to the static electric field induced by effective optical field.

Afterward, it was assumed that this field aligns defects originating from trapping levels and finally creates recording

of space field distribution. But the absolute value of the induced electric strength does not exceed 1 V/cm, which is too small to align defect states. So several authors^{6,7} decided to use conception of charge density asymmetry caused by asymmetric photoionization due to multiphoton excitation. In our opinion, a more appropriate explanation may be the idea of self-organization for the transition dipole moments proposed by Antonyuk et al.^{8,9} Particularly, a model of charge transfer excitons was introduced. In ref 10, it was shown that a substantial role of the photoinduced quasiphonons substantially rescaled the observed phenomenon. Particularly, the photo-induced piezoelectric and electrostricted quasiphonons may play a crucial role for organic chromophores incorporated within the polymer matrices.^{11,12}

From this point of view, chromophores possessing transition metals may be of particular interest because they possess relatively localized d states. Among the transition metals, Ru and Cr derivatives may be of particular interest.

So in the present work we will explore $\chi^{(2)}$ grating and associated second-order optical effects in Ru–alkynyl complexes incorporated within the polymer polymethyl methacrylate (PMMA) matrices. In section 2, main details devoted to sample preparation are given. Section 3 is devoted to measurement setup

and aspects of the phenomenon under observation. Section 4 presents main experimental results including the time kinetics of phenomenon and superposition of external field.

2. Experimental Details

Sample Preparation. The syntheses of alkynyl complexes **C1** and **C2–4** (see Figure 1) follow the literature procedures of Dixneuf.¹³ The preparation of the new alkynes (**A1** and **A2–4**) follows the procedure outlined in Figure 1. Sonogashira coupling¹⁴ was employed to obtain the trimethylsilyl-protected alkynes **Si1–4** in good yields, which were then reacted in the standard manner to give the terminal alkynes **A1–4**. Isolation of the trimethylsilyl-protected alkyne intermediates **Si2–4** offered no advantage in terms of yield and purity. Conversely, a great advantage in purity and yield of the final product **A1** was gained by isolating the trimethylsilyl-protected alkyne **Si1** and reacting it with the arene chrome tricarbonyl phosphonate anion (Horner–Emmons–Wadsworth coupling) prior to the deprotection step. Reaction of this anion with the terminal alkynes **1** afforded a lower yield of **3**, along with several unidentified byproducts. These new alkynes were fully characterized by classical methods.

Reaction of $[\text{RuCl}(\text{dppe})_2][\text{TfO}]$ and these terminal alkynes in dichloromethane at room temperature (r.t.) afforded vinylidene species. These products were not isolated but instead deprotonated with base in situ (using triethylamine) to afford the desired alkynyl complex **C1–4** in good yield (65%). The new alkynyl complexes were characterized by liquid secondary ion mass spectrometry (LSIMS), UV–vis, IR, ^1H , ^{31}P , and ^{13}C NMR spectroscopy. The LSIMS mass spectra of **C2–4** contain molecular ions with fragmentation proceeding by competitive loss of chloro and alkynyl ligands to afford the base peak corresponding to $[\text{Ru}(\text{dppe})_2]$. Fragmentation of **C1** proceeded also by loss of the $\text{Cr}(\text{CO})_3$ group. The IR spectra contain characteristic bands assigned to $\nu(\text{C}\equiv\text{C})$ close to 2035 (**C2–4**) and 2040 cm^{-1} (**C1**). The ^{31}P NMR spectra contain singlet resonances close to 50 ppm, confirming the mutually *trans* stereochemistry of the chloro and alkynyl ligands. The IR spectra of complexes **C2–4** contain characteristic bands assigned to $\nu(\text{C}=\text{O})$ close to 1590 cm^{-1} . Their ^1H NMR spectra contain the characteristic signals from the formyl groups close to 10 ppm. The ^{13}C NMR spectra also contain downfield resonances at 190 ppm consistent with the formyl moiety. Complex **C1**, of low solubility, was degraded gradually in solution. We could not obtain satisfactory ^{13}C spectra in this series. Meanwhile, the η^6 arene complexation is supported by the upfield shift of the arene proton in the ^1H NMR spectra of these complexes and confirmed by characteristic infrared bands assigned to $\nu(\text{C}\equiv\text{O})$ close to 1960 and 1900 cm^{-1} .

The obtained compounds were incorporated into the PMMA matrix. The investigated samples were prepared as a mixture of 4 g of PMMA and 0.035 g of chromophore dissolved in 30 mL of chloroform in the argon atmosphere.

This mixture was mixed using a magnetical stirrer, and afterward they were put in the Alumina tige. By verification of the evaporation rate after the 24 h, samples were obtained under the investigations.

One of the problems of the complexes investigated is their photodestruction under the light influence. The specially performed NMR and IR investigations have shown that under the influence of light, particularly of a power density higher than 450 MW/cm^2 , there occurs a partial destruction of the chromophore; however, in the PMMA matrix, this degradation does not exceed 7.2%, and most of the molecule participates in the desirable processes.

The chemical structure of studied compounds and their UV spectra are presented in Figure 1c.

3. Optical Poling of Ru-Derivative Chromophores

The optical poling has substantial advantages compared to electric-field or corona poling consisting of satisfying phase-matching conditions without the necessity of using electrodes. Contrary to the azo dye chromophores,¹⁵ the investigated composites do not break their structure due to orientation relaxation. At the same time, they possess low mobility of the carriers due to the presence of the d states.

So we try using the guest–host technique similar to that described in ref 16 both to improve the stability of the grating process and to enhance its efficiency, which should be manifested through the decrease of time during which the optical poling process achieves its saturation, determined by corresponding steady-state processes. Simultaneously, we search materials possessing a higher time of $\chi^{(2)}$ grating decay.

The optical poling method consists of two stages: at the first stage, a composite sample is optically treated by the bicolor coherent light. The $\chi^{(2)}$ grating of the DC electric field with the proper wave vector $\mathbf{K} = \mathbf{k}_{2\omega} - 2\mathbf{k}_\omega$ is created by coherent interaction of the fundamental and doubled frequency of the same laser source. The resulting DC field is asymmetric in space and results in appearance of the static electric field.¹⁷ At the second stage, we continue the grating process by one of them, particularly by the doubled frequency beam.

Experimental Details. The optically induced experiment was similar to that described in ref 9 (see Figure 2). The axial symmetry beam sequence of the fundamental $\text{YAlO}_3:\text{Er}^{3+}$ laser ($\lambda = 1.88 \mu\text{m}$ $\text{Er}^{3+} \ ^3\text{H}_4 \rightarrow \ ^3\text{H}_6$ transitions) and its doubled harmonic obtained by the KTP crystal that was cut to satisfy phase-matching conditions were focused inside the sample in the form of a ring with a diameter of about 1.0 cm. The choosing of such lasers is caused by a necessity to avoid an overlap between the fundamental and doubled frequency beams with the absorption and luminescent bands. The duration of the pulses was 320 ns, and the pulse energy was varied within 0.3–2.6 mJ during a repetition frequency of about 12 Hz. The fundamental beam was converted into the doubled frequency ($\lambda = 0.94 \mu\text{m}$) with a conversion efficiency of about 31%. The diameter of the incident beams at the focal point was 90–110 μm , and the power density at the waist was about 1.1 and 0.29 GW/cm^2 by fundamental and doubled harmonics, respectively. The set of mirrors and lenses allow operation by the beam parameters, and the shutters switch off several beams at the desired moment of time. By use of the set of lenses, we varied the diameters of the beams and the IR filters served for spectral separation of the 0.94 μm doubled frequency beam from the fundamental ones. The synchronized photomultipliers worked in the fast-response regime (about 0.1 ns) and were connected to the electronic boxcar integrator. The incident angles of the two beams on the sample's surface create a small angle (about 2–3°). This fact allowed us to control the grating period within 5–47 μm . The polarizations of the beams were linear and were directed perpendicularly to the \mathbf{k} wave vector of beam propagation.

During this illumination of composites with coherent bicolor radiation (during the optical preparing of composites), the electrostatic field grating $\mathbf{E}(r)$ and correspondingly the $\chi^{(2)}$ grating were produced in the space region of the beam's overlap.

The conversion of the fundamental frequency beam into the photoinduced SHG output signal takes place on the accumulative $\chi^{(2)}$ grating. The propagation of the photoinduced SHG is in

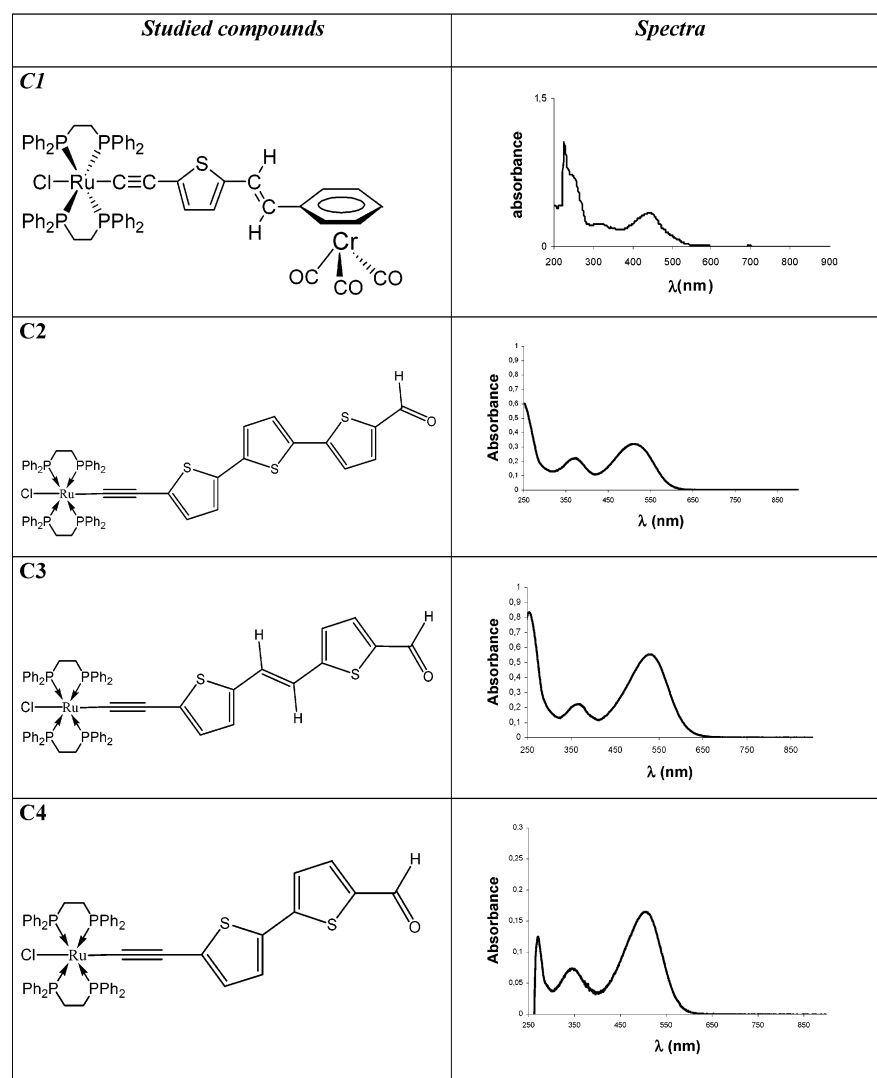
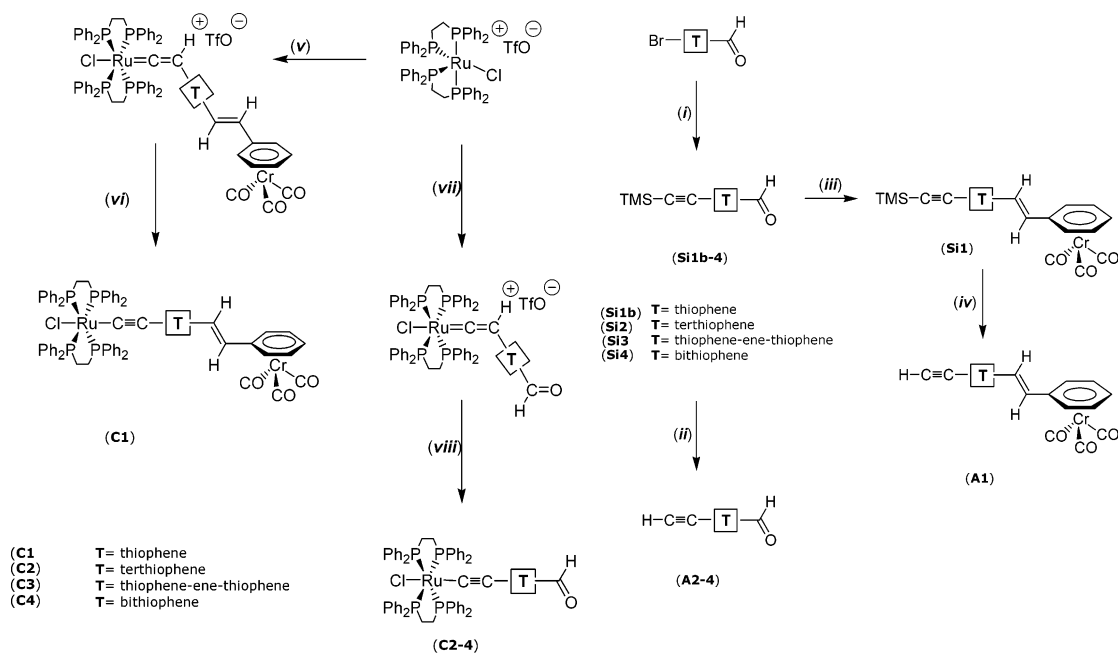


Figure 1. (a) Synthetic procedure to obtain the alkynyl derivatives: (v) $[\text{RuCl}(\text{dppe})_2][\text{TfO}]$ 0.25 mmol, **A1** 0.30 mmol, CH_2Cl_2 40 mL, r.t., 20 h; (vi) 1,8-diazabicyclo[5.4.0]undec-7-ene (DBU) 0.50 mmol, CH_2Cl_2 40 mL, r.t., 1 h; (vii) $[\text{RuCl}(\text{dppe})_2][\text{TfO}]$ 0.50 mmol, **A2–4** 0.60 mmol, CH_2Cl_2 50 mL, r.t., 20 h; (viii) Et_3N 1 mmol, CH_2Cl_2 20 mL, r.t., 1 h. (b) General access to the terminal alkynes **A1–4**: (i) $\text{PdCl}_2(\text{PPh}_3)_2$, CuI, trimethylsilylacetylene, THF, Et_3N , 50 °C, 24 h; (ii) Bu_4NF (solution 1 M in THF), 1 equiv THF, r.t., 1 h; (iii) $[\text{Cr}(\text{CO})_3(\eta^6\text{-C}_6\text{H}_5)\text{CH}_2\text{P}(\text{O})(\text{OCH}_3)_2]$, 1.1 equiv NaH, THF, 12 h, 65 °C; (iv) Bu_4NF (solution 1 M in THF), 2 equiv THF, r.t., 1 h. (c) UV spectra of the Ru chromophore.

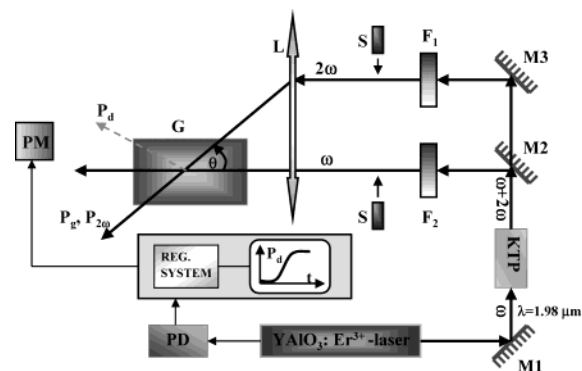


Figure 2. Experimental setup for measurements of optical poling.

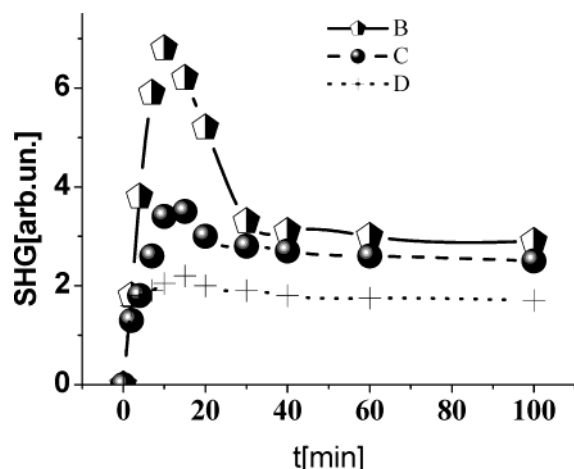


Figure 3. Time kinetics of the SHG for various ratios of power densities for fundamental to writing beams: B, 30; C, 42; D, 16.

the direction of propagation of the incident beam with the doubled frequency (the so-called writing beam). For the registration of the $\chi^{(2)}$ grating itself, we eliminated the incident (writing beam) 2ω signal at the entrance of the sample for short periods (about 0.1 s every 2–3 min). Finally we monitored the peak power $I_{\text{SHG}}(2\omega)$ on the $\chi^{(2)}$ grating using as a detector a photomultiplier in the remote zone. The output photoinduced SHG signals were statistically averaged over 50 SHG pulses to reduce the influence of the SHG signal instability. Independently, instability of the source laser was monitored by an independent fast-time photodiode. The sensitivity of the setup by laser powers was about $0.12 \mu\text{W}/\text{pulse}$.

The setup was supplied additionally by a phase contrast microscopic setup allowing us to monitor the changes of the phase during the optical poling.

4. Results and Discussion

We have found that a sufficiently good photoinduced SHG signal was obtained only for the samples C4 and C3. In the two remaining samples, the output signal was comparable with the scattering background.

From Figure 3, one can see typical dependence of the photoinduced SHG for the C4. One can see that the maximal increase of the output photoinduced SHG is observed during the first 1–12 min. The obtained output photoinduced SHG, which is equal to about 10% compared to the fundamental beam power, is higher than that for the inorganic glasses treated at the same conditions and only a little less than that in the azo dye chromophore. The evaluated maximum second-order susceptibility is equal to about $1.96 \text{ pm}/\text{V}$. The optimal ratio

between the fundamental and the doubled frequency writing beam corresponding to maximal output SHG was equal about 30. A deviation from this ratio in both directions does not give sufficiently good results. The temporary asymmetry may indicate a substantial role of the nonequilibrium processes, described in ref 6.

The direct observation of the $\chi^{(2)}$ process is given in the phase contrast electronic microscopic pictures presented in Figure 4. By comparison of parts a–d of Figure 4 corresponding to different stages of treatment, one can clearly see an occurrence of typical $\chi^{(2)}$ grating fringes. The rings are most clear at the times of 10–12 min, which correlates with the grating observed by the photoinduced PISHG. So one can say that we have shown a correlation between the $\chi^{(2)}$ grating observed by the PISHG and observed by the direct phase contrast electronic microscopy method. The estimated coherence length of the process is about 0.12–0.14 mm. The crucial point is that with increasing time of treatment by the writing beam one can observe more clear fringes corresponding to occurrence of the $\chi^{(2)}$ grating.

Another interesting fact consists of the occurrence of additional rings, which seem like higher harmonics of the fundamental grating. This may be a consequence of the substantial role of the photoinduced polarons determining the process of the grating. Occurrence of the periodical fringes may reflect a substantial role of the d states in the chromophore because for the chromophore without the d states the picture is not so clear. To the best of our knowledge, it is a first direct observation of correlation between the optical grating and output PISHG. It may be a consequence of good photocontrast in the observed materials.

To study the relaxation stability of the composites, we have investigated a decay of the output PISHG with time. In Figure 5 are presented the corresponding dependences vs the number of laser shots in the 125 Hz pulse repetition regime (samples C4 and C3). One can see that, for the optimal fundamental/writing beam ratio (about 30), the output SHG (d_{eff}) does not decrease below the $0.82 \text{ pm}/\text{V}$ (C4) and $0.75 \text{ pm}/\text{V}$ (C3) with respect to the initial noncentrosymmetric grating. For the higher ratios, these decays are substantially higher. So one can conclude that this ratio plays a substantial role in the observed stability of the composites.

At the same time, direction of the electrical field alignment is maximally parallel to the directions of the dipole moments. Because the molecules are prevalingly linearly prolonged, one can expect that the corresponding directions should be parallel. The observed process of the photoinduced SHG has traditional behavior, like in refs 18–21. The efficiency of the photoinduced SHG increases with phototreatment time and reaches the certain steady-state value corresponding to maximum. However, there is a region of the values of $I_2(2\omega)$ for which the efficiency of the SHG increases with time in the initial moment, but further, the signal of the SHG decreases with time and reaches the same steady-state value which is smaller than the maximum magnitude of the photoinduced SHG. This will be the subject of a separate work in future.

We have also done an additional experiment that consisted of the study of the influence of a strong external electric field (up to $10^4 \text{ V}/\text{cm}$) on the optical poling. We have found (see Figure 6) that after switching off the writing beam (2ω) during optical decay, application of a strong electric field (at 75 and 162 min) leads to a jump of the photoinduced SHG with the following decay. Moreover, this effect was observed every time during the repeating process. This may be explained within the framework of theory developed for the self-organized systems.^{5,6}

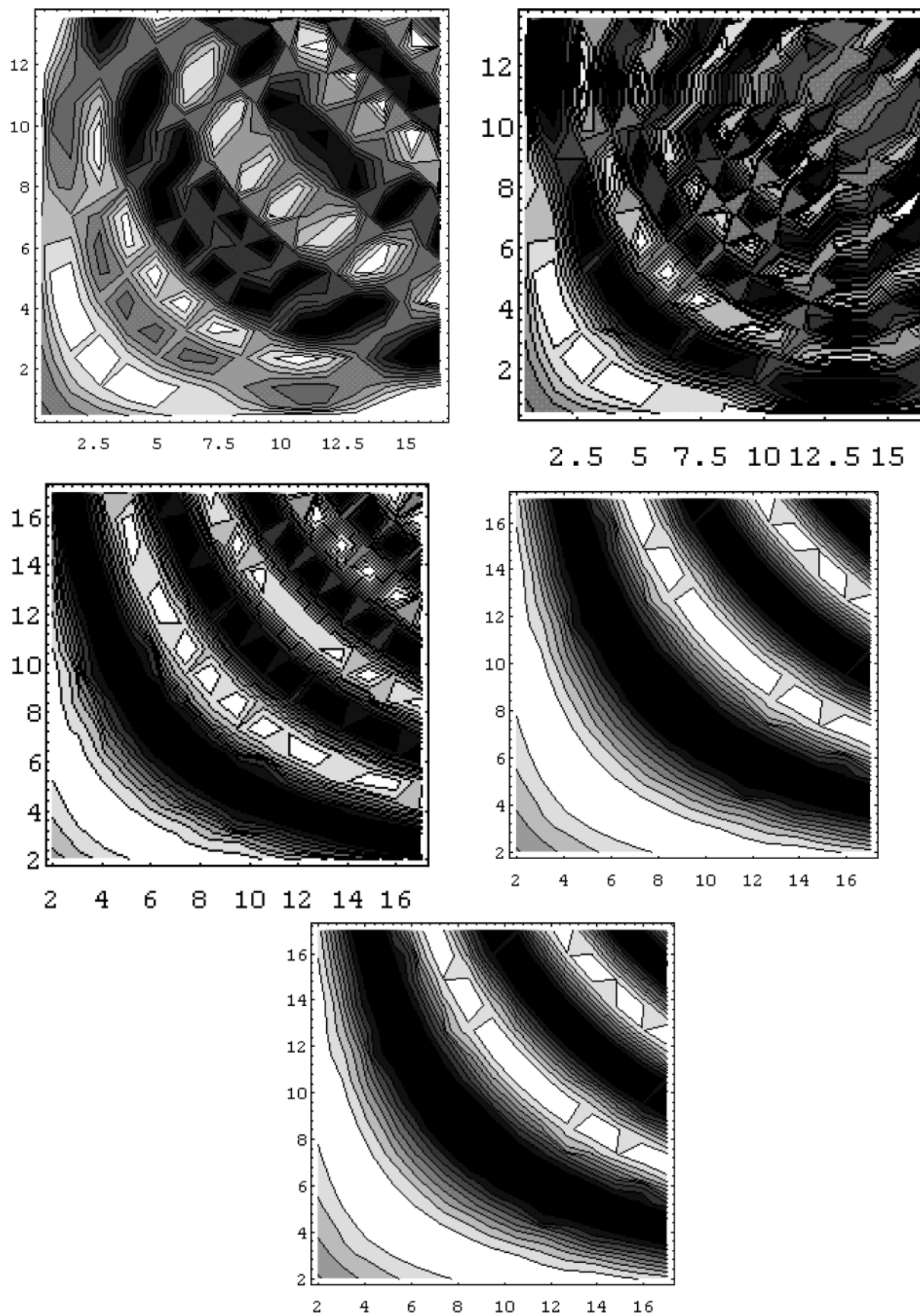


Figure 4. (a) The picture of grating after 2 min of optical treatment. The scale is given in μm . (b) The same after 3 min. (c) After 6 min. (d) After 8 min. (e) After 12 min.

Similar dependences were observed in ref 22. Within the framework of this approach, every excitation of the system with low mobility, to which belongs the considered Ru-derivative

composites, leads to the appearance of nonequilibrium states, which according to the theory are responsible for the phenomenon observed.

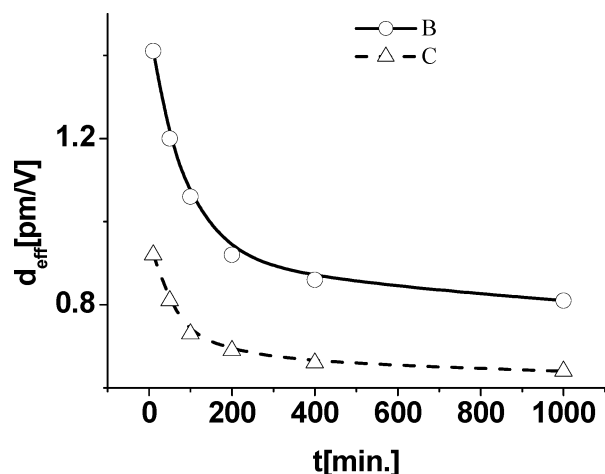


Figure 5. Time decay of the photoinduced SHG after switching off the writing beam field for the sample C4 (B) and C3 (C).

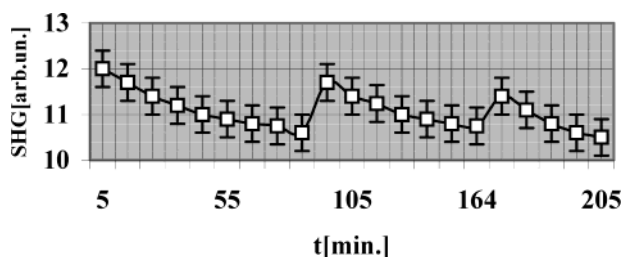


Figure 6. Behavior of SHG after application of the strong electrostatic field (about 10^4 V/cm).

However, in our case, we have a lot of excited trapping levels originating from unoccupied Ru d states. So application of the strong electric field during a short period should lead to recharging of the states and their partial occupation. So in the moment of applying the strong electric field, the effect is reanimated. The general formalism should be similar to that during optical poling, because in both cases, we deal with electric strength; however, the origin of the field will be different in the two cases.

One of possible mechanisms for explaining the long-lived kinetics of the absorption of light in the region of induced high electric field, in our opinion, can be an occurrence of the electrostricted phonons and diffusion processes effectively depopulating the appropriate trapping levels. The major role in the observed kinetics should be played by phonons created by the large photoinduced electric field, eq 3. The corresponding effect is an electrostricted effect described by a fourth-rank γ_{ijkl} tensor and is allowed by symmetry in the disordered media

$$\sigma_{ij} = E_{ijkl} E_k^{(0)} E_l^{(0)} \quad (3)$$

The mechanical stress second-rank tensor σ_{ij} induces a phonon displacement field with the displacement vectors directed along the i and j directions. Because of light polarization, the ionic displacement (determined by phonons) will be different for the two light polarizations (for parallel and perpendicular directions with respect to the incident light). The considered phonons interact with the localized trapping states, changing substantially their living times and polarizabilities. Particularly, there occur the long-lived polaron (autolocalized phonon) states causing an anisotropy of diffusion coefficients D . Its value depends on the type of chromophore.

During the illumination by the polarized light, the diffusion coefficient D of the bound electron-phonon carriers decreases,

favoring additional polarization of the excited trapping levels. The appearance of an additional number of trapping levels leads to the occurrence of the larger number of the delocalized states within the forbidden energy gap, which are responsible for the appearance of the long-lived excitons, determining the phenomenon.

5. Conclusions

In conclusion, in the present paper, we have shown that in the Ru-derivative chromophores the effective maximally achieved second-order optical susceptibility for the wavelength $1.89 \mu\text{m}$ is about 1.94 pm/V . We have revealed that maximal increase of the output photoinduced SHG is observed during the first 1–12 min. The obtained output photoinduced SHG, which is equal to about 10% compared with the fundamental beam power, is higher than that for the inorganic glasses treated at the same conditions and only a little less than in the azo dye chromophore. The optimal ratio between the fundamental and doubled frequency writing beam corresponding to maximal output SHG was equal to about 30. We have shown that for the optimal fundamental/writing beam ratio (about 30) the output SHG (d_{eff}) does not decrease below 0.82 pm/V (C4) and 0.75 pm/V (C3) with respect to the initial noncentrosymmetric grating. We have found also that after switching off the writing beam (2ω) during optical decay, application of a strong electric field (up to 10^4 V/cm) leads to a jump of the PISHG with the following decay.

References and Notes

- Fujii, Y.; Kawasaki, B. S.; Hill, K. O. Sum-Frequency Generation in Optical Fibers. *Opt. Lett.* **1980**, *5*, 48.
- Osterberg, U.; Marquils, W. Dye Laser Pumped by Nd:Yag Laser Pulses Frequency Doubled in a Glass Optical Fiber. *Opt. Lett.* **1986**, *11*, 515.
- Kityk, I. V. *J. Phys.: Condens. Matter* **1994**, *6*, 4199.
- Stolen, Q. H.; Tom, H. W. K. Self-Organized Phase-Matched Harmonic Generation in Optical Fibres. *Opt. Lett.* **1987**, *12*, 585.
- Kityk, I. V. *Tech. Phys. Lett.* **1992**, *18*, 417.
- Baranova, N. B.; Chudinov, A. N.; Zel'dovich, B. Yt. *Opt. Commun.* **1990**, *79*, 116.
- Dianov, E. M.; Starodubov, D. S. *Opt. Fiber Technol.* **1994**, *1*, 3.
- Antonyuk, B. P.; Antonyuk, V. B. *Phys.-Usp.* **2001**, *44*, 53.
- Antonyuk, B. P.; Antonyuk, V. B.; Frolov, A. A. *Opt. Commun.* **2000**, *174*, 427.
- Balakirev, M. K.; Kityk, I. V.; Smirnov, V. A.; Vostrikova, L. I. *Phys. Rev.* **2003**, *A67*, 023806.
- Ozga, K.; Gondek, E.; Danel, A.; Chaczatryan, K. *Opt. Commun.* **2004**, *231*, 437.
- Kityk, I. V.; Makowska-Janusik, M.; Gondek, E.; Krzeminska, L.; Danel, A.; Plucinski, K. J.; Benet, S.; Sahraoui, B. Optical Poling of Oligoether Acrylate Photopolymers Doped by Stilbene-Benzozate Derivative Chromophores. *J. Phys.: Condens. Matter* **2004**, *16*, 231–239.
- (a) Touchard, D.; Haquette, P.; Daridor, A.; Romero, A.; Dixneuf, P. H. *Organometallics* **1998**, *17*, 3844. (b) Touchard, D.; Dixneuf, P. H. *Coord. Chem. Rev.* **1998**, *178–180*, 409.
- (a) Sonogashira, K.; Yatake, T.; Tohda, Y.; Takahashi, S.; Hagihara, N. *J. Chem. Soc., Chem. Commun.* **1977**, 291. (b) Sonogashira, K.; Fujikura, Y.; Yatake, T.; Takahashi, S.; Hagihara, N. *J. Organomet. Chem.* **1978**, *145*, 101. (c) Müller, T. J. *J. Tetrahedron Lett.* **1997**, *38*, 1025. (d) Müller, T. J. *J. Organomet. Chem.* **1999**, *578*, 95.
- Charra, F.; Kajzar, F.; Nunzi, J.-M.; Raimond, F.; Idiart, E. *Opt. Lett.* **1993**, *18*, 419.
- Sahraoui, B.; Kityk, I. V.; Nguyen Phu, X.; Hudhomme, P.; Gorgues, A. *Phys. Rev.* **1999**, *B59*, 9229.
- Antonyuk, B. P.; Novikova, N. N.; Didenko, N. V.; Akstipetrov, O. A. *Phys. Lett.* **2002**, *A298*, 405–409.
- Martin, G.; Toussaere, E.; Griscon, L.; Soulier, E. *Zyss J.* **2002**, *127*, 139.
- Lopez-Logo, E.; Courders, V.; Griscom, L.; Smektaloa, F.; Barthelemy, A. *Opt. Mater.* **2001**, *16*, 413.
- Churikov, V. M.; Hsu, C.-C. *Opt. Commun.* **2001**, *190*, 367.
- Matsuoka, N.; Kitaoka, K.; Si, J.; Fujita, K.; Hirao, K. *Opt. Commun.* **2000**, *185*, 467.
- Kazansky, P. G.; Pruneri, V. *Phys. Rev. Lett.* **1997**, *78*, 2956.